Composites: Part A 192 (2025) 108725

Contents lists available at ScienceDirect

Composites Part A

journal homepage: www.elsevier.com/locate/compositesa

Performance of In-situ Automated Fibre Placement Parts

Ashley R. Chadwick [a,*], Georg Doll [a], Ulrich Christ [b], Sabrina Maier [b], Sylvia Lansky [b]

[a] DLR - Institute for Structures and Design, Pfaffenwaldring 38-40, 70569 Stuttgart, Germany
[b] WIWeb, 85424 Erding, Germany

ARTICLE INFO

Keywords:
AFP
Thermoplastic composites
Mechanical properties

ABSTRACT

Despite being a relatively mature manufacturing technology, in-situ automated fibre placement is still yet to see industrial implementation for the manufacturing of primary and secondary aircraft structures owing to fears of high porosity and inferior mechanical properties. In this study, carbon fibre-reinforced PPS is used as a reference material, with which several laminates are manufactured both in-situ and as preforms for subsequent press consolidation. The mechanical, thermal, and tomography results reveal that for the correct manufacturing process parameters, in-situ laminates from can outperform pressed laminates in certain areas and reach 90% of their performance in others. The porosity is also seen to reduce during the manufacturing process, decreasing to 1.1% from the unprocessed prepreg material 2.2%. These results indicate a promising future for the inclusion of in-situ parts in the coming generations of transport vehicles.

1. Introduction

The implementation of carbon fibre-reinforced polymer (CFRP) structural components in aircraft and spacecraft is nothing new, having been carried out over the past several decades. These efforts, particularly concerning the substitution of classical metallic components, have enabled significant advances in terms of both strength-to-weight and performance output of the vehicles as a whole. However, the advantages of these new components, though significant, have always been overshadowed by a factor of almost equal standing in the aerospace industry; cost. For several years, the need to employ hand-layup techniques to realise composite structures severely limited their application viability. With the advent of fibre winding and Automated Fibre Placement (AFP) technology, significant advances were made in the rate of production, though manual operations to perform bagging prior to autoclave consolidated persisted. While such activities may be considered inherent to thermoset material, where resin curing or infusion is required to develop the binding matrix, thermoplastic–matrix composites should, in theory, be able to avoid such steps, with matrix consolidation possible at the moment of material melting and fusion. The fact that post-layup autoclave (or thermo-forming) consolidation remains the default approach for AFP-manufactured thermoplastic structures [1–3] is a result of the immaturity of the process, specifically an inability to realise comparable mechanical performance using the AFP process alone (“in-situ” manufacturing).

Numerous investigations into the mechanical performance of AFP-produced parts have been conducted [4–13] and while each investigation shares certain common traits, the overall commonality between studies is low. Lamontia et al. [4], Khan et al. [5], and Van Hoa et al. [8] investigated the mechanical performance of manufactured laminates using the “original” configuration of an AFP facility, with a hot (nitrogen) gas torch providing heat to melt the prepreg material matrix. These three studies focused on different aspects of mechanical performance, being quasi-isotropic strength (tension and compression), interlaminar shear strength (ILSS), and unidirectional strength (tension and compression), respectively. Comer et al. [6], Stokes-Griffin and Compston [7], Chen et al. [9], Chadwick et al. [10], and Zhao et al. [12] utilised a more “modern” AFP facility setup to manufacture laminates, with heating provided by a high-powered laser. The mechanical properties investigated in these studies were also varied, ranging from ILSS to Open Hole Compression (OHC) and fibre-perpendicular tensile strength ($\sigma_{t,90}$). Within these studies, fibre-reinforced polyether ether ketone (CF-PEEK) was by far the most extensively investigated [4–8,14] owing to its high mechanical and thermal performance and thus status as the standard thermoplastic CFRP material for aerospace applications. By comparison, fibre-reinforced polyphenylene sulphide (CF-PPS) has seen fewer investigations [9,11,12,15] to ascertain the mechanical performance of AFP-produced parts.

Tables 1 and 2 list mechanical properties for in-situ and fully consolidated (autoclave or hot-press) samples tested within various studies for CF-PEEK and CF-PPS, respectively. As can be seen, a general trend of consolidated laminates outperforming in-situ laminates is observed. This is expected owing to the uniform heating of bulk consolidation processes providing both greater homogeneity and a higher degree of

* Corresponding author.
E-mail address: ashley.chadwick@dlr.de (A.R. Chadwick).

https://doi.org/10.1016/j.compositesa.2025.108725
Received 3 June 2024; Received in revised form 10 January 2025; Accepted 13 January 2025
Available online 30 January 2025

Table 1
Reported mechanical performance for AFP-produced CF-PEEK laminates (in-situ) and laminates produced using a hot press or autoclave (consolidated).

Property		In-situ	Consolidated
Strength [MPa]			
Inter-laminar shear [5–7]	τ_{ILSS}	40.0–98.0	94.8–112.0
Laminar shear [8,14]	τ_{lam}	98.0	80.0
Tensile, 0° [8]	$\sigma_{t,0}$	2420.0	2446.0
Compressive, 0° [8,14]	$\sigma_{c,0}$	1036.0	1407.0
Tensile, QI [16]	$\sigma_{t,*}$	–	850.0
Compressive, QI [4,16]	$\sigma_{c,*}$	462.0	501.0–530.0
Open hole tension [4]	OHT	359.0	359.0
Open hole compression [4,6]	OHC	248.0–255.0	316.0–337.0
Bearing (in tension) [17]	$\sigma_{t,B}$	–	332.0–496.0
Toughness [J/mm^2]			
Fracture toughness [16]	G_{1c}	–	1180.0
Modulus [GPa]			
Laminar shear [8,14]	G_{lam}	5.3	5.5
Tensile, 0° [8,14]	$E_{t,0}$	165.0	136.0
Compressive, 0° [8,14]	$E_{c,0}$	144.0	123.0
Tensile, QI	$E_{t,*}$	–	–
Compressive, QI [4]	$E_{c,*}$	43.4	46.9
OHT	E_{OHT}	–	–
OHC [4]	E_{OHC}	40.7	44.1

Table 2
Reported mechanical performance for AFP-produced CF-PPS laminates (in-situ) and laminates produced using a hot press or autoclave (consolidated).

Property		In-situ	Consolidated
Strength [MPa]			
Inter-laminar shear [9,11,12,15]	τ_{ILSS}	49.4–61.4	66.1–73.9
Tensile, 0° [15]	$\sigma_{t,0}$	–	1912.6
Tensile, 90° [15,18,19]	$\sigma_{t,90}$	–	33.2–42.7
Tensile, QI [20]	$\sigma_{t,*}$	–	793.8
Toughness [J/mm^2]			
Fracture toughness [12,18]	G_{1c}	2970.0	590.0
Modulus [GPa]			
Tensile, 90° [18,19]	$E_{t,90}$	–	4.8–10.8

crystallinity than localised AFP manufacturing [6,9,16]. However, the aforementioned differences in the AFP facilities coupled with further differences in the respective consolidation processes (temperature, pressure, and duration), not to mention variation in the same composite prepreg material from different suppliers, restrict the summary of Tables 1 and 2 to an implicit guide rather than explicit reference.

The work presented here hence aims to reconcile two shortcomings in the current database. Firstly, to provide a comprehensive characterisation of a given material under set conditions and secondly, to broaden the design options available for next-generation AFP-manufactured components by focusing on CF-PPS as opposed to CF-PEEK. CF-PPS has enjoyed recent interest in AFP-manufactured structures [9–13,21] due to its comparable matrix mechanical properties. Additionally, while the glass and melting temperatures of CF-PPS prepreg material are approximately 55 °C and 65 °C lower than CF-PEEK, respectively, CF-PPS is considerately cheaper, making it an attractive candidate for low-temperature (<90 °C applications). Previous investigations by the authors of this work explored the moderation of composite crystallinity and mechanical properties of CF-PPS laminates through characterisations of mechanical performance [10] and the microscopic morphology [21]. The work presented here is considered a direct extension of these previous efforts.

1.1. Novelty

A comprehensive characterisation of the mechanical performance of CF-PPS using both in-situ AFP and hot press forming processes. A complimentary investigation into other relevant part properties, specifically crystallinity and porosity.

Table 3
Physical and thermal properties of CF-PPS material [10].

Property [Unit]	Value
w [mm]	3 × 12.7
t [mm]	0.19
v_f [%]	55
T_g [°C]	89.6
T_c [°C]	122.9/242.3
T_m [°C]	280.4
X_c [%]	14.3

Table 4
Processing parameter values for laminate production.

Parameter [Unit]	Value
T_{tool} [°C]	250
T_{np} [°C]	410
p_{roll} [bar]	6
v_{layup} [m/min]	7.5

Table 5
Laminate layups and associated standards investigated.

Layup	Property	Standard
$[0]_{11}$	τ_{ILSS}	DIN EN 2563
	$\sigma_{t,0}$	DIN EN 2561
	$\sigma_{c,0}$	DIN EN ISO 14126 A1
	$\sigma_{t,90}$	DIN EN 2597 B
$[0, 45, 90, -45]_{2s}$	$\sigma_{t,*}$	DIN EN 2561
	$\sigma_{c,*}$	DIN EN ISO 14126 A1
$[0, 45, 90, -45]_{3s}$	$\sigma_{t,B}$	DIN 65562
	σ_{CAI}	DIN ISO 18356

2. Methodology

Materials and sample production

Tables 3 and 4 list the prepreg material properties and processing parameters used within this work, respectively. Three half-inch (12.7 mm) tapes were deposited simultaneously onto a heated tooling surface (250 °C) using a Multi-Tape Laying Head (MTLH) at a speed of 7.5 m/min. This speed is seen as mid-range within the scope of the reported literature (3–12 m/min [4–9,12]) and has previously been demonstrated to provide a good compromise between the rate of manufacturing and the bonding strength of deposited material layers (plies) [22]. In contrast, the tooling temperature (T_{tool}) is on the upper end of those utilised by other researchers (40 °C–300 °C [5,6,8,9,12]), though all works agree that, in general, a higher tooling temperature leads to increased final part performance through reduced internal stresses and increased crystallinity [10,12]. The nip-point temperature (T_{np}) for this work was set to 410 °C, provided by a 6 kW near-infrared laser as per the facility description in previous works [10,22].

Mechanical characterisation

Using this material and processing parameters a total of six laminates were produced, divided into three layup categories as detailed in Table 5. All laminates had a common length (fibre-parallel) and width (fibre-perpendicular) of 428 mm and 648 mm, respectively, and a thickness ranging from 2.0 mm to 4.5 mm depending on the layup. For each layup, one laminate was trimmed directly following manufacturing to produce the in-situ samples while others were bulk consolidated in a hot-press at 320 °C and 20 bar for 25 min. The cooling rate from the melting temperature down to room temperature was 8 °C/min.

The mechanical properties in investigated, as well as the standards with which they were obtained, are also listed in Table 5. Mechanical

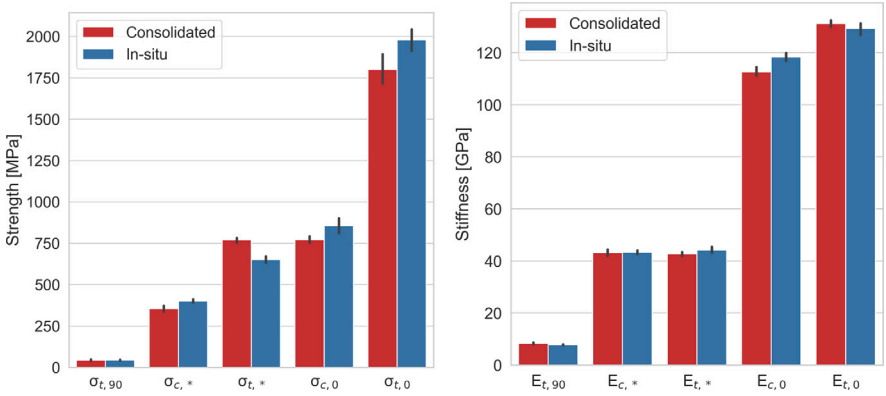

Fig. 1. Tensile and compressive strength (left) and stiffness (right) of in-situ and consolidated samples.

tests were conducted at the Bundeswehr Research Institute for Materials, Fuels and Lubricants (WIWeB Wehrwissenschaftliches Institut für Werk- und Betriebsstoffe) using a universal testing machine. Tensile and compressive tests were performed to simple sample failure as per standard practice. For the ILSS samples, values presented in this work correlate to the maximum force recorded during testing. While there remains debate as to the suitability of short beam shear testing to thermoplastic composite materials, this standard and approach was selected to provide the most direct comparison with other similar studies [6,7]. Bearing strength ($\sigma_{t,B}$) tests were performed (in tension) using a single pin of diameter 6.3 mm and Compression After Impact (CAI) tests were conducted following a range of impact energies up to 70 J.

Thermal characterisation

Sample crystallinity was measured using a DSC214 Polyma Differential Scanning Calorimeter (DSC) using a heating and cooling rate of 10 °C/min in a nitrogen environment. An average sample mass of 9.0 g was used for the measurements. Sample specific enthalpy values were determined using a linear baseline and temperature range of 220–300 °C for the polymer melting reaction.

Computed tomography

Computed tomogrophy (CT) was also carried out at the WIWeB facility, with samples selected from the unprocessed tape as well as the $[0]_{11}$ and $[0,45,90,-45]_{3s}$ laminates. For each laminate, in-situ and consolidated conditions were investigated using an extremely high resolution of 2.5 μm; less than the diameter of a single fibre. The sample volume for the CT measurements ranged from 3.5 mm^3 for the unprocessed tape to 70–150 mm^3 for the $[0]_{11}$ and $[0,45,90,-45]_{3s}$ laminates, respectively. The difference in the sample volume is a simple result of the material thickness with no impact on the subsequent calculation of porosity.

3. Results

Mechanical performance

Fig. 1 shows the mechanical performance of the in-situ and consolidated laminates under tensile and compressive loading, while Fig. 2 shows the response curves of the two configurations to shear loading. Table 6 summarises the majority of the static mechanical results for a direct numerical comparison.

As can be seen, the final performances of in-situ and consolidated CF-PPS laminates were very similar, with most properties agreeing within 10% of one another. Exceptions to this were the interlaminar shear strength and quasi-isotropic tensile strength, which showed a 23.8% and 18.1% improvement following consolidation, respectively. Compressive strength values (both unidirectional and quasi-isotropic) were also higher for in-situ conditions. In assessing the stiffness of the laminates, in-situ and consolidated manufacturing approaches delivered an almost indistinguishable difference with a maximum deviation of 6.4% and a fairly equivalent number of "wins" over each other.

Table 6
Summary of mechanical performance of AFP-produced CF-PPS laminates; in-situ and consolidated post-manufacturing.

Property	In-situ	Consolidated	Change [%]
Strength [MPa]			
τ_{ILSS}	77.2 (± 1.2)	95.6 (± 1.4)	+23.8
$\sigma_{t,0}$	1980.0 (± 95.9)	1799.6 (± 139.3)	−9.1
$\sigma_{c,0}$	856.2 (± 65.7)	771.8 (± 26.0)	−9.9
$\sigma_{t,90}$	43.5 (± 3.3)	44.4 (± 5.5)	+2.1
$\sigma_{t,*}$	651.9 (± 31.2)	770.2 (± 23.5)	+18.1
$\sigma_{c,*}$	399.8 (± 16.4)	361.3 (± 19.4)	−9.6
$\sigma_{t,B}$	473.0 (± 26.8)	531.1 (± 43.9)	+12.3
Modulus [GPa]			
$E_{t,0}$	129.3 (± 3.2)	131.2 (± 1.9)	+1.5
$E_{c,0}$	118.3 (± 2.4)	112.7 (± 2.0)	−4.7
$E_{t,90}$	7.8 (± 0.2)	8.3 (± 0.5)	+6.4
$E_{t,*}$	43.3 (± 1.1)	43.1 (± 1.9)	−0.5
$E_{c,*}$	44.1 (± 1.8)	42.6 (± 0.9)	−3.4

Fig. 3 shows the response of the laminates to different impact energies. The profiles of in-situ and consolidated laminate samples were fairly similar of the range of energies investigated. The consolidated configuration delivered a consistently higher failure stress, with the in-situ alternative a close second with 84%–92% of the consolidated values over the given range.

Fig. 4 summarises the overall mechanical performance of the in-situ and consolidated laminates visually, highlighting that they are indeed very similar to one another. Taking an average value for all recorded properties, the relative strength and stiffness performance of in-situ and consolidated CF-PPS was within 4.0% and 0.14% of each other, respectively. This is significantly less than that of CF-PEEK as observed through the literature (Table 1), which showed a 27.3% and 2.4% discrepancy for strength and stiffness, respectively. Comparing mechanical properties obtained within this study with those from Table 2 shows very good agreement between the two, as summarised in Table 7.

The following section of this work focuses on explaining the similarities between the in-situ and consolidated performance of CF-PPS with a focus on two important composite structure criteria; crystallinity and porosity.

Crystallinity and porosity

Fig. 5 shows the measured DSC profiles for the two extreme thickness cases within this study, $[0]_{11}$ and $[0,45,90,-45]_{3s}$, for both in-situ

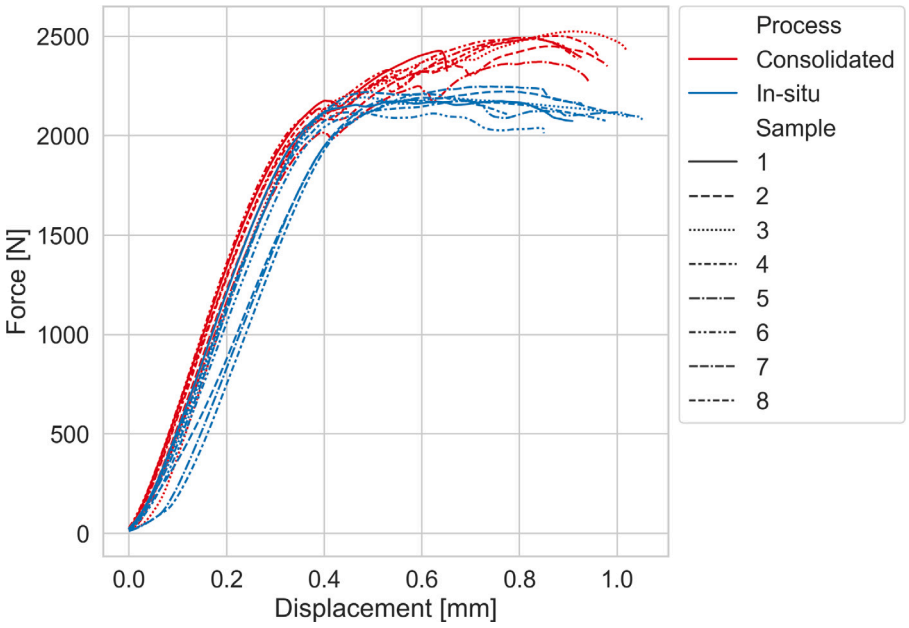

Fig. 2. Comparative ILSS force and displacement profiles for in-situ and consolidated sample series.

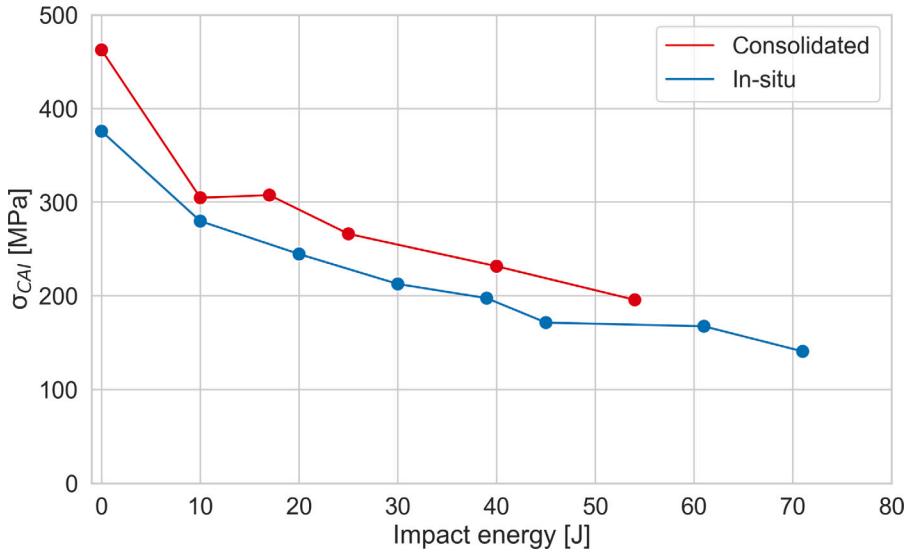

Fig. 3. Compression after impact behaviour of in-situ and consolidated laminates.

Table 7
Comparative performance of CF-PPS laminates from this study from those from available literature.

Property	In-situ		Consolidated	
	This study	Literature	This study	Literature
Strength [MPa]				
τ_{ILSS}	77.2	61.4	95.6	73.9
$\sigma_{t,0}$	1980	–	1799.6	1912.6
$\sigma_{t,90}$	43.5	–	44.4	42.7
$\sigma_{t,*}$	651.9	–	770.2	793.8
Modulus [GPa]				
$E_{t,90}$	7.8	–	8.3	10.8

and consolidated configurations. The in-situ $[0]_{11}$ condition shows the characteristic second peak in response to the elevated tool temperature (as reported in detail in a previous study [10]), though the visibility of this peek is lost in the $[0, 45, 90, -45]_{3s}$ laminate owing to the increased number of plies (with increasing distance from the tool surface). As can be seen, the layup seems to have a minimal influence on the DSC profile and recorded melting temperature. However, in-situ laminates yielded T_m values slightly lower than that of the unprocessed material as given in Table 3, while consolidated samples yielded a slightly higher value.

Fig. 6 shows bulk crystallinity values obtained from DSC measurements, where in-situ laminates exhibited crystallinities of 30.3% and 28.9% for the unidirectional and quasi-isotropic layups, respectively. The slight discrepancy in crystallinity (<1%) given the twofold difference in thickness for the two layup configurations is not considered significant and hence stable crystallinity values are deemed achievable using in-situ manufacturing within this study. The measured crystallinites increased to 33.2% and 31.2% following consolidation, indicating that the processing parameters used within this study, specifically the tooling temperature, allowed in-situ laminates to achieve more than 90% of the maximum consolidated value, thus supporting

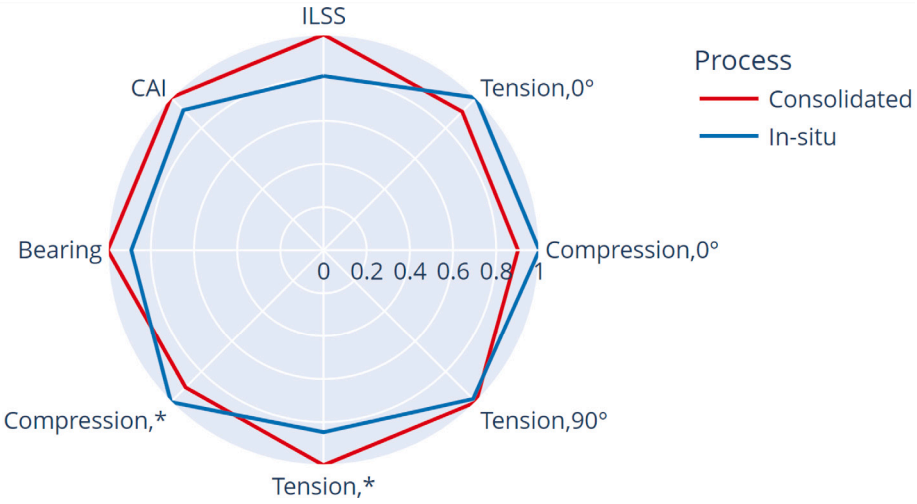

Fig. 4. Normalised mechanical performance of in-situ and consolidated laminates.

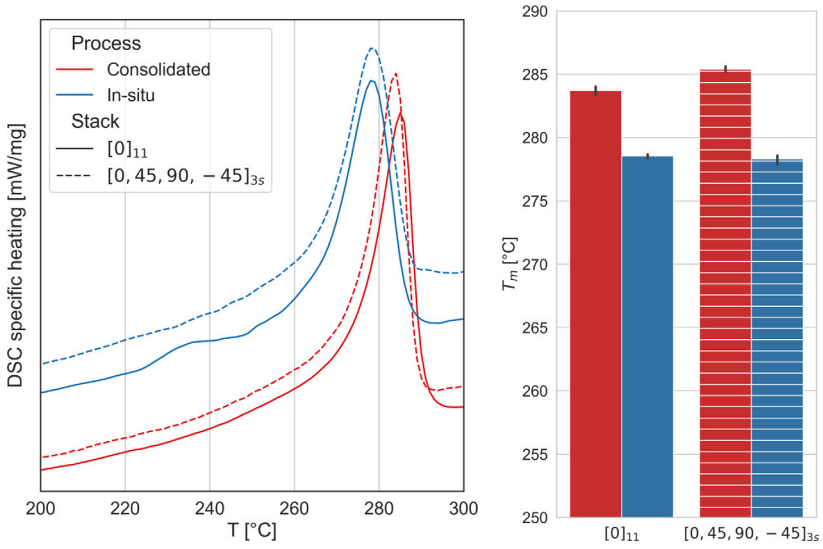

Fig. 5. Measured DSC profiles of laminates (left) and observed changes in the measured melting temperature (right).

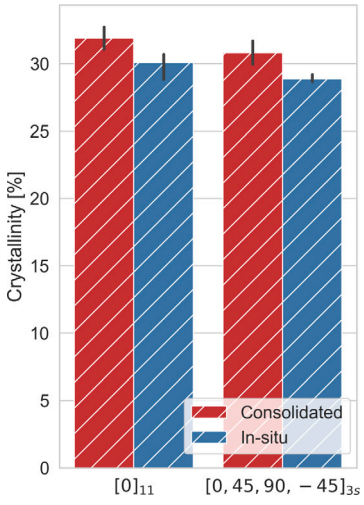

Fig. 6. Measured crystallinity of in-situ and consolidated laminates.

the observed similarities in mechanical performance.

Table 8 lists the porosity of samples as determined by the CT-analysis. The unprocessed tape featured the highest value of 2.2%, with all laminates exhibiting at least a 50% reduction in bulk porosity through the manufacturing process. While there is evidence in the literature of reductions in total part porosity following AFP manufacturing [5,23,24], many studies neglect to measure the porosity of the unprocessed material, making most observations somewhat circumstantial. For the purpose of this investigation it is sufficient to say that a reduction from the original prepreg value was consistently observed for all manufactured laminates, regardless of thickness or layup. Furthermore, post-manufacturing consolidation in the hot press essentially eliminated porosity altogether, as is expected (Fig. 7). While these integral values are surely useful for assessing total part porosity, a closer look at the CT data yields a deeper insight into the nature of porosity as influenced by the AFP process.

Fig. 8 illustrates the form and alignment of voids exemplarily in the $[0, 45, 90, -45]_{3s}$ in-situ laminate, while Fig. 9 shows the through-thickness void content of the same laminate considering the fibre angle of the layup. As can be seen, the orientation of the voids correlate very strongly with fibre angle and, as an extension, the orientation of the ply in the laminate layup. It should be noted that the vectoring approach

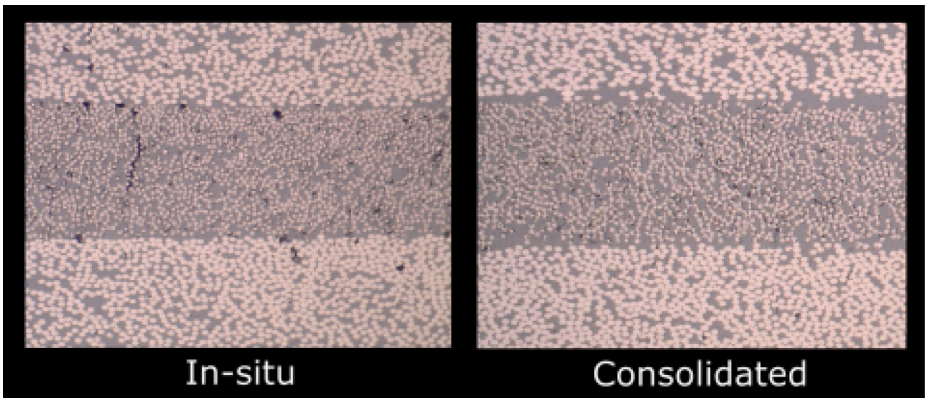

Fig. 7. Comparative void presence in $[0, 45, 90, -45]_{3s}$ laminates before and after press consolidation.

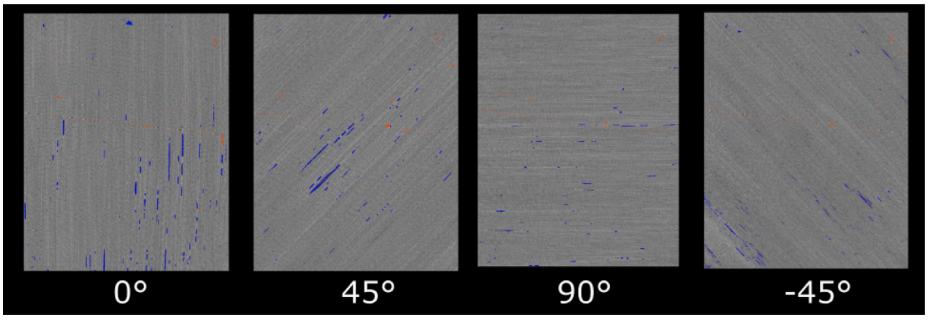

Fig. 8. Representative shape and alignment of voids in the variously oriented plies (as observed in the $[0, 45, 90, -45]_{3s}$ in-situ laminate).

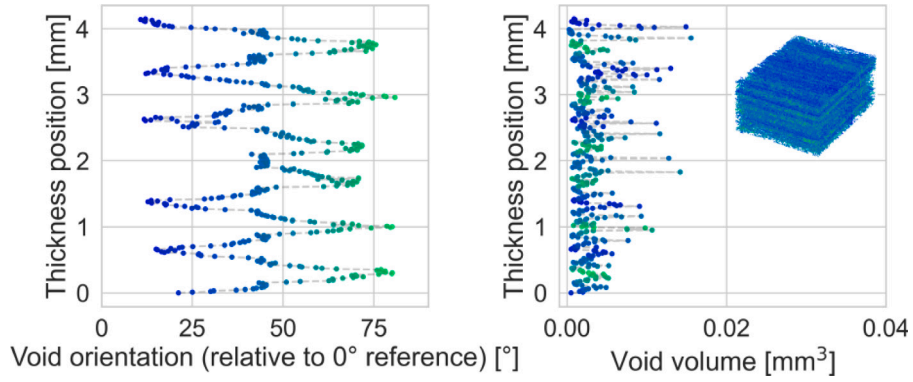

Fig. 9. Void content and orientation in the through-thickness direction for the $[0, 45, 90, -45]_{3s}$ in-situ laminate.

Table 8
CT-measured porosity of unprocessed tape and subsequent laminates.

Layup	Porosity [%]		
	Tape	In-situ	Consolidated
$[0]_{11}$	2.2	1.11	0.00
$[0, 45, 90, -45]_{3s}$	2.2	1.10	0.02

used to calculate the void angle over- and under-estimates the angle of 0° and 90° voids, respectively, resulting in deviations from the expected maximum and minimum values. This approach does however serve to highlight the nature of voids in the produced laminates.

This through-thickness analysis was applied to both unidirectional and quasi-isotropic laminates, as well as the unprocessed tape, as shown in Fig. 10. It was observed that the void content of the unprocessed tape is fairly uniform, with slightly lower values at the tape surface on both sides. In contrast, both laminates show a somewhat tapering profile, with a lower void content on the lower (tool) side of the laminate and a higher content on the upper side of the laminate. This behaviour is significantly more pronounced for the $[0]_{11}$ laminate, which is understandable given the lack of fibre variation thus allowing sequentially deposited plies to merge with one another as the fibres intermingle in the interlaminar zone. Furthermore, the areas of low void content on the lower side of the laminate are significantly lower than the unprocessed tape values, supporting the assumption of compaction of the voids during the AFP process. The appearance of high values very close to the tool side can be attributed to a first ply material known to be more porous than the laminate material. Similarly low values are observed locally in the $[0, 45, 90, -45]_{3s}$ as well, though given the 45° angle between subsequent plies, the same level of compaction of the unidirectional laminate was not observed.

Finally, Fig. 11 shows the relations between individual void volume and the total sample void volume, individual void volume and the total void count, and the sphericity of the voids within the samples. Using these three characteristics, the following observations can be made:

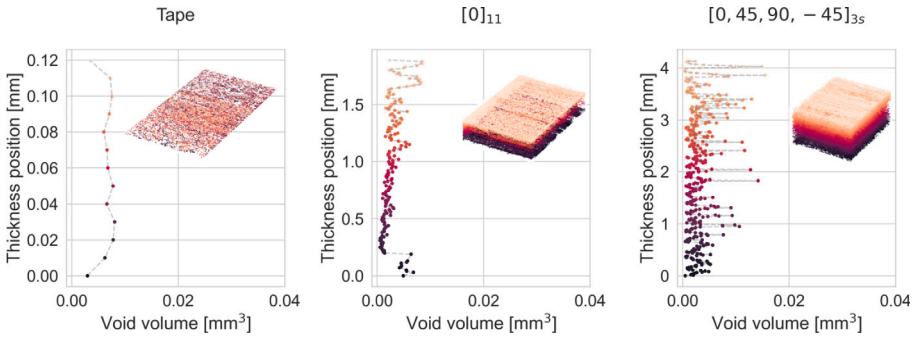

Fig. 10. Void content in the through-thickness direction.

Firstly, the largest voids observed in the manufactured laminates are larger than those in the unprocessed tape material; up to an order of magnitude. This result is of interest given that the overall porosity of the laminates was observed to be lower that the unprocessed tape. Secondly, the distribution of voids in all samples is drastically skewed towards small pores ($<10^{-5}$ mm^3), such that less than 10% of the total void population is responsible for up to 70% of the total void volume. Finally, the sphericity of the voids in all samples decrease with increasing void volume, indicating that the majority of individually resolved voids are small and spherical in nature, with larger voids being more cylindrical in nature, as shown in Fig. 8.

4. Discussion

From the combination of mechanical, thermal, and optical analyses performed within this study, a comprehensive understanding of AFP-manufactured laminates is possible. The mechanical performance of the in-situ laminates was very similar to their consolidated counterparts, typically within 10%. This is a noteworthy result considering the measured crystallinity and porosity of in-situ laminates were lower and higher, respectively, which has to-date been a popular argument for excluding AFP-produced parts from consideration for primary structures. However, the quantified performance profile of CF-PPS produced using in-situ AFP makes a strong case for inclusion in future structures.

It should be noted that a direct comparison between the various investigative techniques described in this work should be undertaken with some caution owing to the significant variance in scale. For example, while the choice to perform CT scans with 2.5 μm resolution was chosen to provide the greatest possible detail regarding the part porosity, the respective volume of CT samples compared to mechanical samples are orders of magnitude smaller. It is therefore possible that a more comprehensive understanding of the laminate characteristics may be further developed in subsequent works. As a result, the work presented here is considered an incremental rather than conclusive investigation into the performance of CF-PPS.

Fig. 12 shows the comparative performance of CF-PPS and CF-PEEK laminates based on the values of Tables 1 and 6. Values of bearing strength yielded the most positive result for CF-PPS, with both in-situ and consolidated values outperforming their CF-PEEK counterparts. Tension, compression, and ILSS results, on the other hand, typically placed CF-PPS between 60% and 90% of CF-PEEK (consolidated) values. It should however be noted that the fibre volume of the CF-PPS samples was 55% as opposed to the 60% of CF-PEEK literature values. It should also be noted that the agreement between CF-PPS and CF-PEEK for the in-situ configuration was very good despite the disparity in polymer mechanical properties. A more comprehensive comparison would require CF-PEEK samples manufactured and tested within the same controlled environment.

Extrapolating the results of this investigation to a more industrial scale, ie large part production, does of course raise the issue of how toolings may be designed to achieve the high temperatures required to improve part mechanical properties. While this is a separate topic in and of itself, the authors of this work are involved in such activities and would stress that prospective heated toolings need only provide a hot surface (in contact with the composite first ply) rather than heat

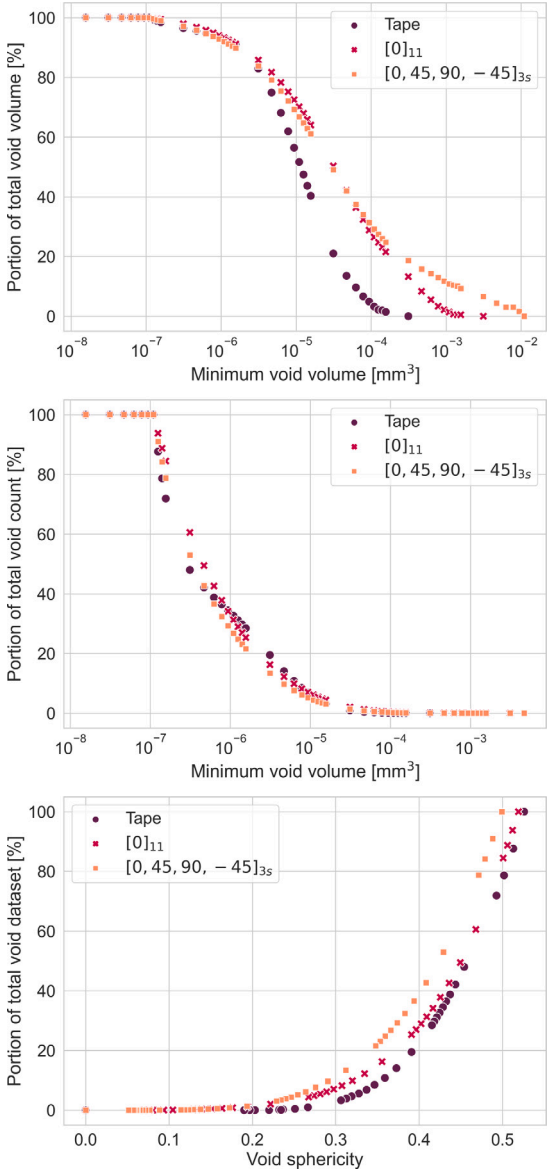

Fig. 11. Analysis of the void volume (top), void population count (centre), and void sphericity (bottom) for the tape and in-situ laminates.

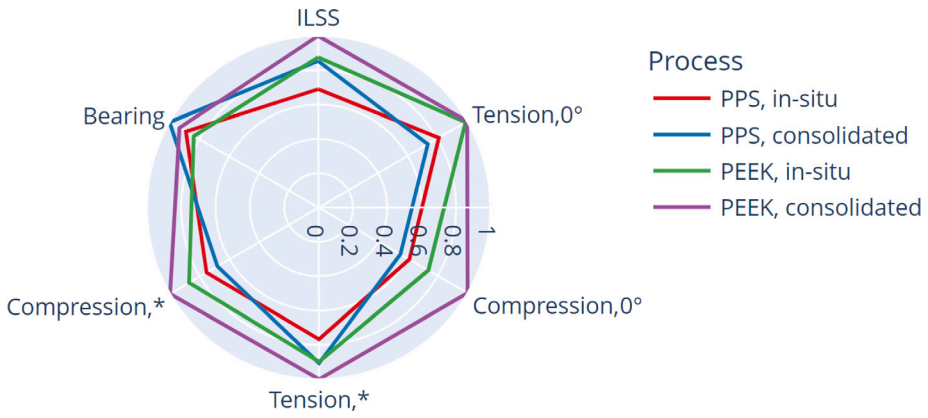

Fig. 12. Comparison of mechanical strength of CF-PPS (this study) and CF-PEEK (from literature [4,8,14,16,17]) using AFP.

the entire tool. The selection of heating elements (geometry and heat transfer method), insulation materials, and load-bearing structures (to resist the consolidation roller) thus form the central design criteria in designing toolings to take advantage of the results presented in this work.

5. Conclusion

This study has performed a detailed and thorough characterisation of CF-PPS as manufactured using AFP, both in-situ and with subsequent consolidation post-layup. The mechanical analysis revealed that in-situ mechanical properties typically achieved 80%–90% of those exhibited by post-consolidated laminates. Certain mechanical properties, such as 0° compression and tension, were even higher for the in-situ configuration. The stiffness of samples displayed a negligible difference with respect to the manufacturing method. The crystallinity of in-situ samples were also very similar to the consolidated samples and the bulk porosity of in-situ laminated was less than 1.2%. This represents a significant reduction from the unprocessed material porosity of 2.2%. An in-depth analysis of CT data of the unprocessed tape and in-situ samples yielded interesting insight into the distribution of porosity within the tape as well as a tendency for lower porosity on the tooling side of the in-situ laminates (for both unidirectional and quasiisotropic) layups. This thorough characterisation is intended to provide current, reliable mechanical properties for the design of future aircraft structures for which CF-PPS is a promising candidate. Furthermore, this work has shown that for the correct manufacturing configuration, in-situ CF-PPS laminates can perform similarly or above those produced using traditionally thermoformed methods, enabling new opportunities for high-speed additive manufacturing of composites.

CRediT authorship contribution statement

Ashley R. Chadwick: Writing – review & editing, Writing – original draft, Visualization, Methodology, Investigation, Formal analysis, Data curation, Conceptualization. **Georg Doll:** Writing – review & editing, Resources, Project administration, Funding acquisition. **Ulrich Christ:** Writing – review & editing, Methodology, Formal analysis. **Sabrina Maier:** Methodology, Formal analysis. **Sylvia Lansky:** Methodology, Formal analysis.

Declaration of competing interest

The authors declare the following financial interests/personal relationships which may be considered as potential competing interests: Dr. Ashley R. Chadwick reports financial support was provided by German Federal Ministry of Defence. If there are other authors, they declare that they have no known competing financial interests or personal relationships that could have appeared to influence the work reported in this paper.

Acknowledgement

The authors of this work would like to acknowledge financial support by the German Federal Ministry of Defence.

Data availability

The data that has been used is confidential.

References

[1] Gardiner G. Composites world: PEEK or PEKK in future TPC aerostructures? 2018, URL https://www.compositesworld.com/articles/peek-or-pekk-in-future-tpc-aerostructures. Online Article - Composites World.

[2] Nagelsmit M. Thermoplastic upper spar for an aircraft pylon by automated fibre placement. In: Proceedings of the 39th SAMPE Europe conference. United Kingdom; 2018, p. 1–9.

[3] Omairey SL, Sampethai S, Hans L, Worrall C, Lewis S, Negro D, Sattar T, Ferrera E, Blanco E, Wighton J, Muijs L, Veldman SL, Doldersum M, Tonnaer R, Jayasree N, Kazilas M. Development of innovative automated solutions for the assembly of multifunctional thermoplastic composite fuselage. Int J Adv Manuf Technol 2021;117(5):1721–38. http://dx.doi.org/10.1007/s00170-021-07829-2.

[4] Lamontia M, Funck SB, Gruber MB, Cope RD, Waibel B, Gopez NM. Manufacturing flat and cylindrical laminates and built up structure using automated thermoplastic tape laying, fiber placement, and filament winding. Sampe J 2003;39:30–8.

[5] Khan MA, Mitschang P, Schledjewski R. Identification of some optimal parameters to achieve higher laminate quality through tape placement process. Adv Polym Technol 2010;29(2):98–111. http://dx.doi.org/10.1002/adv.20177.

[6] Comer AJ, Ray D, Obande WO, Jones D, Lyons J, Rosca I, O' Higgins RM, McCarthy MA. Mechanical characterisation of carbon fibre-PEEK manufactured by laser-assisted automated-tape-placement and autoclave. Composites A 2015;69:10–20. http://dx.doi.org/10.1016/j.compositesa.2014.10.003, URL https://www.sciencedirect.com/science/article/pii/S1359835X14003133.

[7] Stokes-Griffin CM, Compston P. The effect of processing temperature and placement rate on the short beam strength of carbon fibre-PEEK manufactured using a laser tape placement process. Composites A 2015;78:274–83. http://dx.doi.org/10.1016/j.compositesa.2015.08.008, URL https://www.sciencedirect.com/science/article/pii/S1359835X15002791.

[8] Van Hoa S, Duc Hoang M, Simpson J. Manufacturing procedure to make flat thermoplastic composite laminates by automated fibre placement and their mechanical properties. J Thermoplast Compos Mater 2016;30(12):1693–712. http://dx.doi.org/10.1177/0892705716662516.

[9] Chen J, Fu K, Li Y. Understanding processing parameter effects for carbon fibre reinforced thermoplastic composites manufactured by laser-assisted automated fibre placement (AFP). Composites A 2021;140:106160. http://dx.doi.org/10.1016/j.compositesa.2020.106160, URL https://www.sciencedirect.com/science/article/pii/S1359835X20303985.

[10] Chadwick AR, Kotzur K, Nowotny S. Moderation of thermoplastic composite crystallinity and mechanical properties through in situ manufacturing and post-manufacturing tempering: Part 1 - mechanical characterisation. Composites A 2021;143:106286. http://dx.doi.org/10.1016/j.compositesa.2021.106286, URL https://www.sciencedirect.com/science/article/pii/S1359835X21000166.

[11] Zhao D, Chen J, Zhang H, Liu W, Yue G, Pan L. Effects of processing parameters on the performance of carbon fiber reinforced polyphenylene sulfide laminates manufactured by laser-assisted automated fiber placement. J Compos Mater 2021;56(3):427–39. http://dx.doi.org/10.1177/0021998321105582 7.

[12] Zhao D, Li Z, Liu W, Li T, Yue G, Pan L. Crystallization mechanism and mechanical properties of CF/PPS thermoplastic composites manufactured by laser-assisted automated fiber placement. J Compos Mater 2022;57(1):49–61. http://dx.doi.org/10.1177/00219983221137676.

[13] Zhao D, Liu W, Chen J, Yue G, Song Q, Yang Y. Interlaminar bonding of high-performance thermoplastic composites during automated fiber placement in-situ consolidation. J Compos Mater 2024;58(20):2247–61. http://dx.doi.org/10.1177/00219983241263808.

[14] Cai X. Determination of process parameters for the manufacturing of thermoplastic composite cones using automated fiber placement (Master's thesis), Concordia University; 2012.

[15] Kang C-S, Shin H-K, Chung Y-S, Seo M-K, Choi B-K. Manufacturing of carbon fibers/polyphenylene sulfide composites via induction-heating molding: Morphology, mechanical properties, and flammability. 2022, http://dx.doi.org/10.3390/polym14214587.

[16] Saito N, Horizono H, Ishikawa N, Takayanagi T, Takeda N, Kojima H. Residual strain monitoring during hot pressung of thermoplastic composites by a distributed fiber optic sensor. In: Proceedings of the 3rd ITHEC. 2016.

[17] Yao C, Qi Z, Chen W, Zhang C. Effect of CF/PEEK plasticity behavior on the mechanical performance of interference-fit joint. Polym Compos 2021;42(5):2574–88. http://dx.doi.org/10.1002/pc.26003.

[18] Oshima S, Higuchi R, Kato M, Minakuchi S, Yokozeki T, Aoki T. Cooling rate-dependent mechanical properties of polyphenylene sulfide (PPS) and carbon fiber reinforced PPS (CF/PPS). Composites A 2023;164:107250. http://dx.doi.org/10.1016/j.compositesa.2022.107250, URL https://www.sciencedirect.com/science/article/pii/S1359835X22004316.

[19] Taketa I, Kalinka G, Gorbatikh L, Lomov SV, Verpoest I. Influence of cooling rate on the properties of carbon fiber unidirectional composites with polypropylene, polyamide 6, and polyphenylene sulfide matrices. Adv Compos Mater 2020;29(1):101–13. http://dx.doi.org/10.1080/09243046.2019.1651083.

[20] Sharif EA, Razali N, Hamdan H, Ismail N, Shamsullizam NH, Esa MD, Abd Aziz NZ, Mohamad MKA, Rashidi SA. Physical, thermal and mechanical properties of carbon fibre/polyphenylene sulfide (CF/PPS) composite at different tool temperatures fabricated by hot press. J Adv Res Appl Mech 2024;117(1):190–203. http://dx.doi.org/10.37934/aram.117.1.190203, URL https://semarakilmu.com.my/journals/index.php/appl_mech/article/view/4272.

[21] Kotzur K, Chadwick AR, Löbbecke M. Moderation of thermoplastic composite crystallinity and mechanical properties through in-situ manufacturing and post-manufacturing tempering: Part 2 - morphological characterisation. Composites A 2022;163:107225. http://dx.doi.org/10.1016/j.compositesa.2022.107225, URL https://www.sciencedirect.com/science/article/pii/S1359835X22004067.

[22] Dreher P, Chadwick AR, Nowotny S. Optimization of in-situ thermoplasticautomated fiber placement process parameters through DoE. In: Proceedings ofthe 40th SAMPE Europe conference. Nantes, France; 2019, p. 1–13.

[23] Saenz-Castillo D, Martín M, Calvo S, Rodriguez-Lence F, Güemes A. Effect of processing parameters and void content on mechanical properties and NDI of thermoplastic composites. Composites A 2019;121:308–20. http://dx.doi.org/10.1016/j.compositesa.2019.03.035, URL http://www.sciencedirect.com/science/article/pii/S1359835X19301150.

[24] Miao Q, Dai Z, Ma G, Niu F, Wu D. Effect of consolidation force on interlaminar shear strength of CF/PEEK laminates manufactured by laser-assisted forming. Compos Struct 2021;266:113779. http://dx.doi.org/10.1016/j.compstruct.2021.113779, URL https://www.sciencedirect.com/science/article/pii/S0263822321002403.